



## Effect of Surface Sulfonation on the Ordered and Textural Properties of Vanadium and Iron Containing SBA-15

Suna BALCI<sup>1,\*</sup>, Sultan YÜKSEL<sup>1</sup>

<sup>1</sup>Chemical Engineering Department, Gazi University, Ankara, 06570, Turkey

### Article Info

Received: 26/07/2017

Accepted: 09/11/2017

### Keywords

Sulfonation,  
Crystalline structure,  
Pore structure,  
Textural properties

### Abstract

Sulfonation of SBA-15 by use of H<sub>2</sub>SO<sub>4</sub> as the synthesis acid and post surface sulfonation of hydrothermally synthesized V-, Fe-SBA-15 samples with different M/Si mole ratios were carried out by use of dilute sulfuric acid. The doubling of hydrogen ions' amount in case H<sub>2</sub>SO<sub>4</sub> usage led to partial deterioration of the ordered structure. X-ray diffraction patterns showed that the metal loading to SBA-15 matrix caused increases in (100) plane reflections up to four-five times supporting the formation of longer hexagonal arrays. The improved ordered structure of metal-SBA-15 was not destroyed by post-sulfonation. Micro-mesoporus structure of the samples resembled type IV nitrogen isotherm with a H1 hysteresis loop of IUPAC classification. Increase of BET surface area accompanied with around 20% increase in micropore volume took place by metal contribution. Increases both in Saito-Foley (SF) mean micropore and Barrett-Joyner-Halenda (BJH) mean mesopore sizes were designated by the increase of M/Si ratio in the synthesis solution. Around 150-200 m<sup>2</sup>.g<sup>-1</sup> decreases in BET surface area were accompanied by the decreases in the mesopore volume and mean mesopore dimensions, and partly increases in the micropore volume and mean micropore diameters were observed with sulfonation.

## 1. INTRODUCTION

Nanoporous materials whose structural properties are fully designed have important technological application areas such as adsorbents, clean energy storage and catalyst/catalyst support and membrane support. In addition to the properties related with increasing the catalytic activity and selectivity in multiple reaction system, possessing high surface area, adjustable proper pore size distribution and high thermal stability are also required in applications. For the necessity of elimination of diffusion limitations the meso-porous structures, including micropores come to the fore in recent studies.

Micro-mesoporous ordered SBA-15, a member of SBA-n (Santa Barbara Amorphous-n) with high surface area and thicker pore walls is a good candidate as catalyst support. In addition to its one dimensional hexagonal uniform mesopore size distribution which controls the mass transfer and selectivity in multi reaction system, its microporous structure provides the area for reaction. The exhibited high hydrothermal and mechanical stability due to its thicker walls and high surface area caused by the formation of micro-pores in the thick pore wall are the main advantages [Zhao et al., 1998a, b; Meynen et al., 2009]. Although these superior textural properties, it exhibits low catalytic activity due to the neutral surface combination. Catalytic activities of SBA-15 can be improved with some modifications done during and/or after the synthesis. Metal incorporation is one of the most effective of these methods [Taguchi and Schüth, 2005; Chmielarz et al., 2010; Zhang et al., 2012; Hea et al., 2015; Karthikeyan et al., 2016; Chirieac et al., 2016]. The regular sizes channels and the micropores within the silica wall are the advantages of SBA-15 structure although the catalytic activity is concerned. The hydrothermal incorporation of metals has the advantages of both the uniform

\*Corresponding author, e-mail: [sunabalci@gazi.edu.tr](mailto:sunabalci@gazi.edu.tr)

distribution of metal species in the matrix and preservation of the ordered structure in addition to its one-pot synthesis economy.

Iron and vanadium metals are common active species that are used to enhance the activities especially in selective oxidation, dehydration, alkylation of low molecular weight organics [Popova et al., 2009; Hess et al., 2005; Capek et al., 2008; Moreno et al., 2008; Tsoncheva et al., 2008; Gracia et al., 2009; Zhang et al., 2009]. Sulfonation which gives rise in the number of surface functional groups is another technique which is used mostly. The studies in the literature showed that surface sulfonation increased the surface acidity by the adsorption of sulfur groups to metal oxide surfaces [Hua et al., 2001; Kilos et al., 2005; Hess et al., 2005]. Functionalizing the surface can be done by use of sulfur containing compounds during the hydrothermal synthesis. Post modification especially with sulfuric acid treatment of the synthesized sample or impregnation of salts of sulfate to the host are also applicable. The contribution of surface functional groups can be achieved using sulfuric acid or like sulfur containing compounds during the synthesis or post-treatment enhances the catalytic activity by increasing the surface acidity. The regular sizes channels and the micropores within the silica wall are the advantages of SBA-15 structure although the catalytic activity is concerned. Post treatments such as sulfate impregnation limits the activity by hindering the metal active species as it blockage the pore entrance. It was reported that the sulfonated metal supported on mesoporous structures such as  $\gamma\text{Al}_2\text{O}_3$ , MCM-41 or pillared clay exhibited superior catalytic performance [Chen et al., 2001; Mishra and Parida, 2006; Fuxiang et al., 2007; Zhao et al., 2008; Garg et al., 2009].

In this study it was aimed to investigate the effects of metal addition and sulfonation on SBA-15 support. Vanadium and iron containing SBA-15 structures were hydrothermally synthesized and surface sulfonation were performed in one pot synthesis. Sulfuric acid as a sulfonation source was also used as synthesis acid to see its effect on crystalline structure of SBA-15. The surface properties of the samples were investigated.

## 2. MATERIAL and METHOD

The recipe suggested by Zhao and co-workers [1998a] was followed for the synthesis of SBA-15 using sodium silicate as silica source, pluronic123 [amphiphilic triblock copolymer, poly (ethylene glycol)-block-poly (propylene glycol)-block-poly (ethylene glycol)] as surfactant and deionized water as solvent. The host SBA-15 was synthesized by use of synthesis acid as 1M HCl or 1M H<sub>2</sub>SO<sub>4</sub>. One pot synthesis of V- and Fe-SBA-15 samples were carried out with H<sub>2</sub>SO<sub>4</sub> by changing M/Si molar ratios as 0.06 and 0.09 using vanadyl sulphate trihydrate (VOSO<sub>4</sub>.3H<sub>2</sub>O) and iron sulfate dihydrate (FeSO<sub>4</sub>.2H<sub>2</sub>O) as vanadium and iron sources respectively to enhance the surface sulfonation. The separated powders were calcined in an air by a heating rate of 1 °C/min until 550 °C with 6 h dwell time at that temperature. Post surface sulfonation of the synthesized samples was also performed by the treatment of them with dilute (1 M 15 mL/g) sulfuric acid for an hour at room temperature. The sulfonated samples were separated, dried at 100 °C followed by the same calcination steps used in one pot synthesis [Yüksel, 2012].

The powder X-ray diffraction (XRD) patterns of samples were recorded on a Philips PW 3040 diffractometer equipped with CuK $\alpha$  radiation source ( $\lambda=0.15406$  nm) in the  $2\theta$  range of 0.5–90° with a scan speed of 0.025 (s<sup>-1</sup>) and a step size of 0.02 to determine crystalline structure and metal phases. Nitrogen adsorption/desorption isotherms of the samples pre-dried at 373 K and outgassed at 573 K were obtained by means of a Quantochrome Autosorb 1C gas adsorption system at liquid nitrogen temperature within the P/P<sub>0</sub> range of 10<sup>-7</sup>-0.99. The total pore volume ( $V_{\text{total}}$ ), micro+meso pore volume ( $V_{\mu+m}$ ) values were estimated from the desorption data at P/P<sub>0</sub> values of ~ 0.99 and 0.96, respectively. The t-method was used to determine the micropore volume values. BET surface area ( $S_{\text{BET}}$ ) values were calculated within P/P<sub>0</sub> values of 0.05-0.30. The mean micro and meso pore dimensions were read from the maximas of size distributions [Lowell et al., 2006].

### 3. RESULTS and DISCUSSION

The characteristic of long range hexagonally ordered as reflection peak (100) and the other two or three reflection peaks (110), (200), (210) were observed in the sample synthesised by HCl as the synthesis acid as consistent with the literature [Zhao et al., 1998a; Kilos et al., 2005; Zhang et al., 2009, Qiang et al., 2009]. (100), (110) and (200) plane diffractions were seen at  $0.84^\circ$ ,  $1.45^\circ$  and  $1.67^\circ$  Bragg angles (Figure 1). Use of  $H_2SO_4$  as the synthesis acid resulted in small decreases in (100) plane peak intensity which occurred a little lower value while two others were almost destroyed. It was reported that the decrease of pH caused some deformation in the ordered structure [Aktaş et al., 2011]. This distortion was the result of increase of doubling the  $H^+$  ions in the synthesis solution which decreased the pH of the synthesis media.

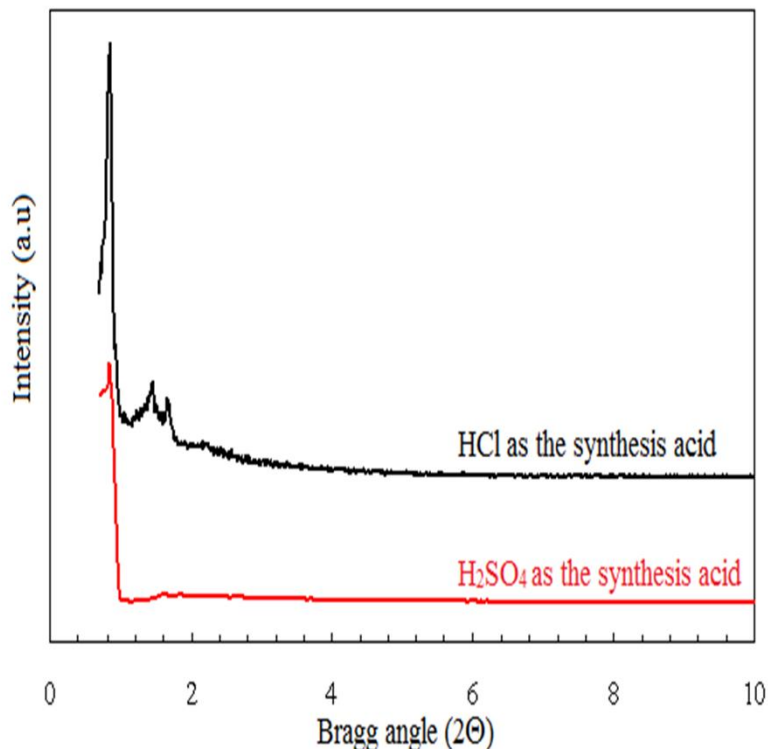


**Figure 1.** XRD patterns of SBA-15 samples

The metal loading resulted in a small shift at the Bragg angle of most prominent characteristics of SBA-15 structure as a result the cell parameter (d spacing - $d_{100}$ , wall thickness- $\delta$ , center to center distance- $a$ ) values were increased a little (Figure 2A, 2B, Table 1). The high increases in (100) diffraction peak's intensity occurred in all cases by metal incorporation. The increase up to four-five times was the confirmation of the formation of long scale ordered structure in addition to the improvements in the textural properties. Diffractions of (110) and (200) planes followed nearly the same pattern for d-spacing shifts as the (100) peaks which defined the hexagonal symmetry in general. Due to the increase of metal concentration, the mechanism of micelle formation could be affected, resulting in the formation of different lengths of hexagonal array template. The diffraction intensity of (110) and (200) planes of vanadium incorporated sample decreased a little by the increase of M/Si ratio while the distortion become evident by use of iron source. It was also seen that post sulfonation did not change the structure of Metal-SBA-15 too much for both metal sources at low M/Si ratio. For high iron loaded sample, the second and third peaks were almost diminished after sulphating as the result of the crystal structure deterioration. In the studies carried out in the literature, crystal structure deterioration and delamination were observed especially in the iron and iron-containing pillared clays [Balci and Gökçay 2002; Moronta et al., 2008, Yuan et al. 2008; Balci and Gökçay, 2009].

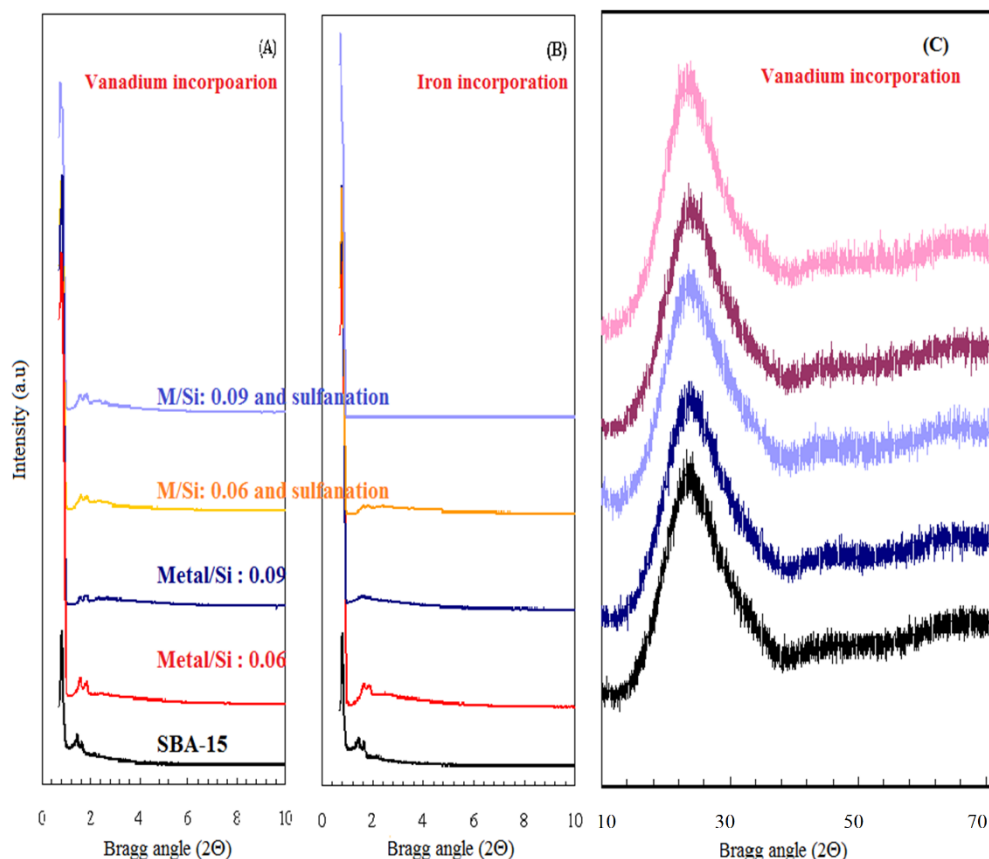


**Figure 2.** XRD patterns of (A) vanadium (B) iron containing samples in the range of 1-10° (C) vanadium containing samples in the range of 10-70°

Support SBA-15 and metal loaded SBA-15 gave similar XRD patterns in Bragg angle range of 10-70° and no obvious diffraction peaks contributing to the crystalline metal/metal oxide and sulfur compounds were not identified in Bragg angle range of 10 – 70°. This could be caused by the well distribution of them within the amorphous silica wall with small sizes that could not be identified by the XRD measurements or low metal loading under severe acidic synthesis environment.

**Table 1.** Structural Properties of Samples

Sample	$d_{100}$ nm	$a$ nm	$\delta$ nm	$S_{BET}$ $m^2 \cdot g^{-1}$	$V_{tot}$ $cm^3 \cdot g^{-1}$	$V_{meso+mic}$ $cm^3 \cdot g^{-1}$	$V_{mic}$ $cm^3 \cdot g^{-1}$	$d_{BJH}$ nm	$d_{SF}$ nm
SBA-15	10.51	12.14	5.41	791	1.13	1.07	0.28	6.73	0.87
V6-SBA-15	10.63	12.27	5.47	808	1.25	1.16	0.33	6.79	0.88
V9-SBA-15	10.76	12.42	5.60	870	1.25	1.13	0.31	6.82	0.86
S@V6-SBA-15	10.76	13.06	6.08	615	1.31	1.28	0.34	7.23	1.01
S@V9-SBA-15	11.32	12.42	5.20	651	1.14	1.10	0.30	6.98	0.99
Fe6-SBA-15	10.76	12.42	5.49	971	1.34	1.29	0.34	7.03	0.87
Fe9-SBA-15	10.89	12.57	5.84	600	1.60	1.11	0.51	6.73	0.95
S@Fe6-SBA-15	10.76	13.06	6.95	675	1.34	1.33	0.45	7.22	0.98
S@Fe9-SBA-15	***	12.42	8.54	509	1.47	1.15	0.44	6.11	0.85

77 K nitrogen adsorption/desorption isotherms of all samples shown in Figure 3 resembled the type IV isotherm with H1 type hysteresis loop based on IUPAC (International Union of Pure and Applied Chemistry) classification corresponding to typical of mesoporous materials which have hexagonal arrays. All samples had high gas adsorption at low relative pressures ( $P/P_0 < 0.02$ ). Increase of BET surface area from  $800 \text{ m}^2 \cdot \text{g}^{-1}$  up to  $970 \text{ m}^2 \cdot \text{g}^{-1}$  and an around 20% increase in micropore volume were observed by metal contribution (Table 1). The iron loading resulted in more enhancement in textural properties consistent with the results of XRD. Higher gas adsorption values especially in mesopore range may be caused by the increase in the length and number of hexagonal arrays after iron incorporation. In the severe acidic synthesis media, the  $(\text{S}^{\circ}\text{H}^+)(\text{X}^-\text{T}^+)$  ionic interaction took place (Zhao et al., 1998b). Here  $\text{I}^+$  was the protonated Si-OH moiety, and  $\text{S}^{\circ}$  and  $\text{X}^-$  represented the nonionic surfactant and halide anion, respectively. It was proposed that metal compounds directed to the surfactant heads resulted in more interaction with silica and surfactant ends hence the settling of silica under this condition led improvements in pore formation.

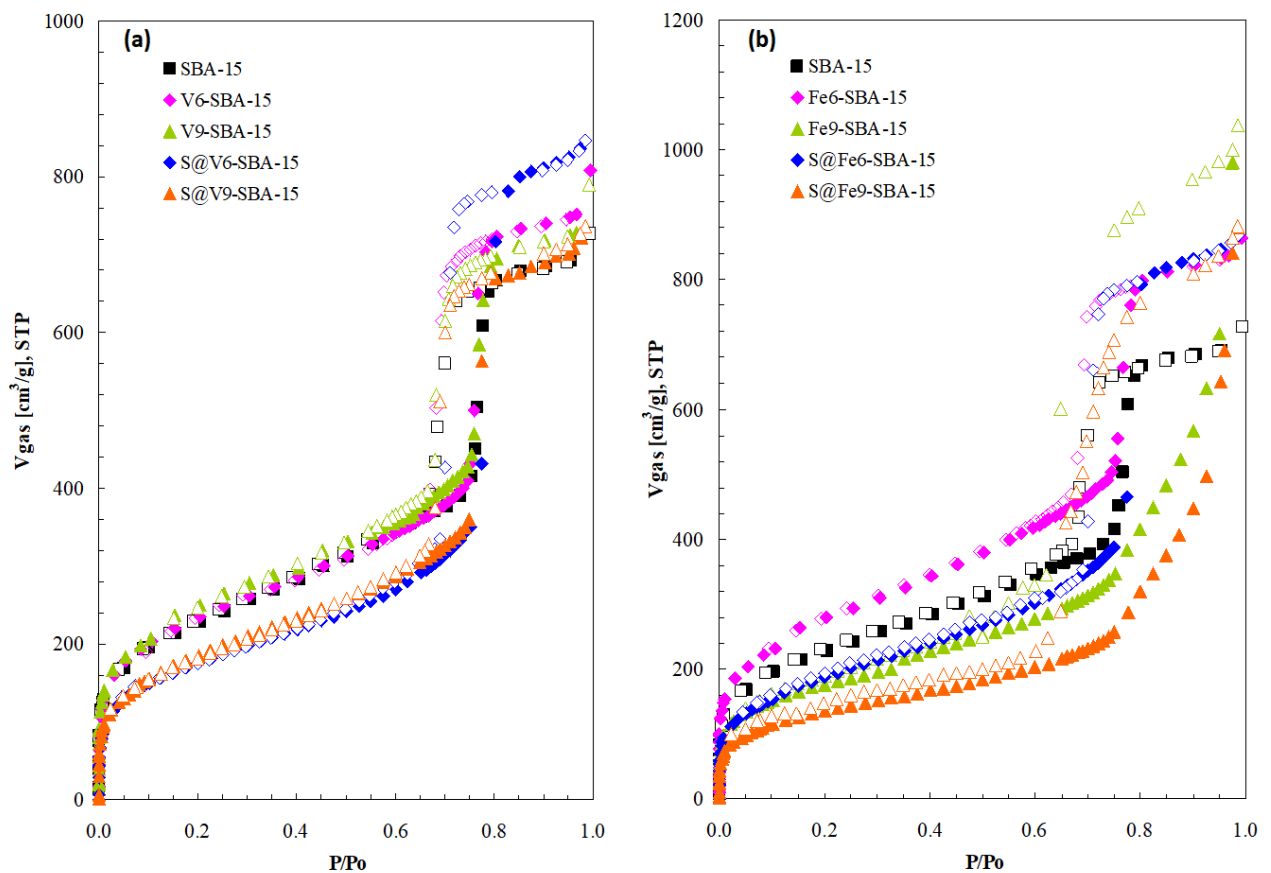


**Figure 3.** 77 K nitrogen adsorption/desorption isotherms of (a) vanadium (b) iron containing SBA-15 samples (S@:sulfanated samples).

Increases in BJH mean mesoporous size and SF mean microporous sizes read from the maxima of poresize distribution curves (Figure 4) were designated by the increase of metal/silica ratio in the synthesis solution. It has been determined that the post sulfation process could lead to the pore deformation and destruction of some pore wall and accordingly, decreases in BET surface area about 20% accompanied by decreases in mesopore volume and mean mesopore dimensions, and partly increases in micropore volume and mean micropore diameters were observed for each sulfanated materials (Table 1). The occurred distortion in the ordered structure seen by XRD (Figure 2B), especially for high iron loaded sample (Fe9-SBA-15), resulted in disturbance in the mesopore size, and the uniform mesopore size distribution (Figure 4) relative to vanadium loaded samples were observed. In the studies carried out in the literature, crystal structure deterioration and delamination

were observed especially in the iron and iron-containing pillared clays [Balci and Gökçay 2002; Moronta et al., 2008, Yuan et al. 2008; Balci and Gökçay, 2009]. In the X-ray diffraction patterns for Fe/Si molar ratio of 0.09 the second and third peaks which were present in other samples in the 1-20<sup>0</sup> Bragg angle range after material sulphating, were not visible. This crystal structure deterioration observed in iron-containing samples showed that the mechanism of micelle formation was affected in the presence of iron.

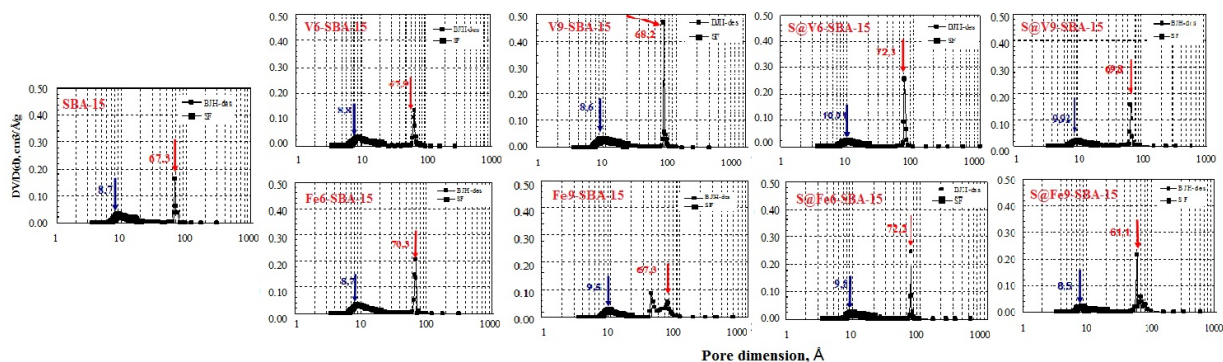


Figure 4. Saito–Foley (SF) micro and Barrett–Joyner–Halenda (BJH) mesopore size distribution of samples

#### 4. CONCLUSIONS

The SBA-15 ordered structure was improved by metal loading showing an increase in the XRD peak intensities. Post sulfonation did not destroy the ordered hexagonality. The well-ordered metal-SBA-15 catalysts having a high surface area were successfully synthesized with surface areas and pore dimensions reaching to 971 m<sup>2</sup>/g and 7.0 nm, respectively. Surface functional groups and metal loading success increased by use of H<sub>2</sub>SO<sub>4</sub> as synthesis acid.

#### ACKNOWLEDGEMENTS

This work was partially supported by Scientific Research Project Department of Gazi University (Project code BAP 06/2009-20).

#### CONFLICT OF INTEREST

No conflict of interest was declared by the authors

#### REFERENCES

- Balci, S., Gökçay, E., “Effects of drying methods and calcination temperature on the physicochemical properties of iron intercalated clays”, *Mater. Chem. Phys.*, 76: 46-51, (2002).
- Balci, S., Gökçay, E., “Pore structure and surface acidity evaluation of Fe-PILCs”, *Turk J. Chem.*, 33: 843-856, (2009).
- Capek, L., Adam, J., Bulanek, L., Kosova, G., Cicmanec, P., Knotek, P., “Oxidative dehydrogenation of ethane over vanadium supported on mesoporous materials of M41S family”, *Appl. Catal. A: Gen.*, 342: 99-106, (2008).

Chen, C.L., Li, T., Cheng, S., Lin, H.P., Bhongale, C.J., Mou, C.Y., “Direct impregnation method for preparing sulfated zirconia supported on mesoporous silica”, *Micropor. Mesopor. Mater.*, 50: 201-208, (2001).

Chirieac, A., Dragoi, B., Ungureanu, A., Ciotonea, C., Mazilu, I., Royer, S., Mamede, A.S., Rombi, E., Ferino, I., Dumitriu, E., “Facile synthesis of highly dispersed and thermally stable copper-based nanoparticles supported on SBA-15 occluded with P123 surfactant for catalytic applications”, *J. Catal.*, 339: 270–283, (2016).

Chmielarz, L., Kus'trowski, P., Dziembaj, R., Cool, P., Vansant, E.F., “SBA-15 mesoporous silica modified with metal oxides by MDD method in the role of DeNOx catalysts”, *Micropor. Mesopor. Mater.*, 127: 133–141, (2010).

Fuxiang, L., Feng, Y., Yongli, L., Ruifeng, L., Kechang, X., “Direct synthesis of Zr-SBA-15 mesoporous molecular sieves with high zirconium loading: Characterization and catalytic performance after sulfated”, *Micropor. Mesopor. Mater.*, 101: 250–255, (2007).

Garg, S., Soni, K., Kumaran, G.M., Bal, R., Gora-Marek, K., Gupta, J.K., Sharma, L.D., Dhar, G.M., “Acidity and catalytic activities of sulfated zirconia inside SBA-1”, *Catal. Today*, 141: 125–129, (2009).

Gracia, M.D., Balu, A.M., Campelo, J.M., Luque, R., Marinas, J.M., Romero, A.A., “Evidences of the in situ generation of highly active Lewis acid species on Zr-SBA-15”, *Appl. Catal. A: Gen.*, 371: 85-91, (2009).

Hea, S., Hea, S., Zhang, L., Li, X., Wang, J., He, D., Lu, J., Luo, Y., “Hydrogen production by ethanol steam reforming over Ni/SBA-15 mesoporous catalysts: Effect of Au addition”, *Catal. Today*, 258: 162–168, (2015).

Hess, C., Drake, I.J., Hoefelmeyer, J.D., Tilley, T.D., Bell, A.T., “Partial oxidation of methanol over highly dispersed vanadia supported on silica SBA-15”, *Catal. Lett.*, 5: 1-8, (2005).

Hua, W., Yue, Y., Gao, Z., “Acidity enhancement of SBA mesoporous molecular sieve by modification with  $\text{SO}_4^{2-}/\text{ZrO}_2$ ”, *J. Molecular Catal. A: Chemical*, 170: 195-202, (2001).

Karthikeyan, S., Pachamuthu, M.P., Isaacs, M.A., Kumar, S., Lee, A.F., Sekaran, G., “Cu and Fe oxides dispersed on SBA-15: A Fenton type bimetallic catalyst for N,N-diethyl-p-phenyl diamine degradation”, *Appl. Catal. B: Environ.*, 199: 323–330, (2016).

Kilos, B., Nowak, I., Ziolk, M., Tuel, A., Volta, J.C., “Transition metal containing (Nb, V, Mo) SBA-15 molecular sieves- synthesis, characteristic and catalytic activity in gas and liquid phase oxidation”, *Stud. Surf. Sci. Catal.*, 158: 1461-1468, (2005).

Lowell, S., Shields, J.E., Thomas, M.A., Thommes, M.M., *Characterization of porous solids and powders: surface area and pore size and density*, Kluwer Academic Publishers, NewYork, , pp. 12, 23, 132, (2006).

Meynen, V., Cool, P., Vansant, E.F., “Verified syntheses of mesoporous materials”, *Micropor. Mesopor. Mater.*, 125: 170–223, (2009).

Mishra, T., Parida, K.M., “Effect of sulfate on the surface and catalytic properties of iron–chromium mixed oxide pillared clay”, *J. Colloid Interface Sci.*, 301: 554–559, (2006).

- Moreno, S., Sanabria, N., Alvarez, A., “Synthesis of pillared bentonite starting from the Al-Fe polymeric precursor in solid state, and its catalytic evaluation in the phenol oxidation reaction”, *Catal. Today*, 133-135: 530-533, (2008).
- Moronta, A., Oberto, T., Carruyo, G., Solano, R., Sanchez, J., Gonzalez, E., Huerta, L., “Isomerization of 1-butene catalyzed by ion-exchanged, pillared and ion exchanged/pillared clays”, *App. Catal. A. General*, 334: 173-178, (2008).
- Aktas, O., Yasyerli, S., Dogu, G., Dogu, T., “Structural variations of MCF and SBA-15-like mesoporous materials as a result of differences in synthesis solution pH”, *Mat. Chem. Phys.*, 131: 151–159, (2011).
- Popova, M., Szegedi, A., Zheleva, C., Mitov, I., Kostova, N., Tsoncheva, T., “Toluene oxidation on titanium- and iron-modified MCM-41 materials”, *J. Hazard. Mater.*, 168, 226–232, (2009).
- Qiang, L., Wen-Zhi, L., Dong, Z., Xi-Feng, Z., “Analytical pyrolysis–gas chromatography/mass spectrometry (Py–GC/MS) of sawdust with Al/SBA-15 catalysts”, *J. Anal. Appl. Pyroly.*, 84: 131–138, (2009).
- Taguchi, A., Schüth, F., “Ordered mesoporous materials in catalysis”, *Micropor. Mesopor. Mater.*, 77: 1–45, (2005).
- Tsoncheva, T., Ivanova, L., Dimitrova, R., Rosenholm, J., “Physicochemical and catalytic properties of grafted vanadium species on different mesoporous silicas”, *J. Colloid Inter. Sci.*, 321: 342-349, (2008).
- Yuan, P., Bergaya, F.A., Tao, Q., “A combined study by XRD, FTIR, TG and HRTEM on the structure of delaminated Fe-intercalated/pillared clay”, *J. Colloid Inter. Sci.*, 324: 142-149, (2008).
- Yüksel, S., Vanadyum ve demir içerikli SBA-15 sentezi ve yüzey sülfatlamasının yapısal özellikler üzerine etkisi, Yüksek Lisans tezi, Gazi Üniversitesi Fen Bilimleri Enstitüsü, , Ankara,(2012).
- Zhang, H., Tang, C., Lv, Y., Sun, C., Gao, F., Dong, L., Chen, Y., “Synthesis, characterization, and catalytic performance of copper-containing SBA-15 in the phenol hydroxylation” *J. Colloid Inter. Sci.*, 380: 16–24, (2012).
- Zhang, Q., Li, Y., An, D., Wang, Y., “Catalytic behavior and kinetic features of FeOx/SBA-15 catalyst for selective oxidation of methane by oxygen”, *Appl. Catal. A: Gen.*, 356: 103–111, (2009).
- Zhao, D., Feng, J., Huo, Q., Melosh, N., Fredrickson, G.H., Chmelka, B.F., Stucky, G.D., “Triblock copolymer syntheses of mesoporous silica with periodic 50 to 300 Angstrom pores”, *Science*, 279:, 548-552, (1998a).
- Zhao D., Huo, Q., Feng, J., Chmelka, B.F., Stucky, G.D., “Nonionic Triblock and Star Diblock Copolymer and Oligomeric Surfactant Syntheses of Highly Ordered, Hydrothermally Stable, Mesoporous Silica Structures”, *J. Am. Chem. Soc.*, 120: 6024–6036, (1998b).
- Zhao, J., Yue, Y., Hua, W., He, H., Gao, Z., “Catalytic activities and properties of sulfated zirconia supported on mesostructured g-Al<sub>2</sub>O<sub>3</sub>, *Appl. Catal. A: Gen.*, 336 (1–2): 133-139, (2008).